

Feedback-enhanced squeezing or cooling of fluctuations in a parametric resonator

Adriano A. Batista

Departamento de Física, Universidade Federal de Campina Grande

Av. Aprígio Veloso 882, Campina Grande-PB, CEP: 58.429-900, Brazil

(Dated: January 14, 2025)

Abstract

Here we analyse ways to achieve deep subthreshold parametric squeezing of fluctuations beyond the -6 dB limit of single degree-of-freedom parametric resonators. One way of accomplishing this is via a lock-in amplifier feedback loop. Initially, we calculate the phase-dependent parametric amplification with feedback of an added ac signal. In one approach, we use the averaging method to obtain the amplification gain, while in the second approach, we obtain the ac response of the parametric amplifier with feedback using the harmonic balance method. In this latter approach, the feedback is proportional to an integral term that emulates the cosine quadrature output of a lock-in amplifier multiplied by a sine at the same tone of the lock-in. We find that the gain obtained via these two methods are the same whenever the integration time span of the integral is a multiple of the tone period. When this is not the case, we can obtain considerable deamplification. Finally, we analyse the response of the parametric resonator with feedback, described by this integro-differential model, to an added white noise in the frequency domain. Using this model we were able to calculate, in addition to squeezing, the noise spectral density in this resonator with feedback. Very strong squeezing or cooling can be obtained.

I. INTRODUCTION

Parametrically driving resonators play an important role in nanomechanical systems [1]. Driving parametrically a resonator is a way to obtain very high effective quality factors [2]. Hence, amplifiers based on these resonators can achieve very high gains and a very narrow gain bandwidth. This narrow band decreases the effect of fluctuations due to added noise. Very sensitive accelerometers [3], force [4] and mass sensors [5, 6] based on these resonators have been implemented experimentally in micro and nanomechanical systems.

Further decrease of fluctuations can be achieved when noise squeezing techniques are used. In a pioneering paper in 1991, Rugar and Grütter [7] experimentally observed thermal noise squeezing in a capacitively actuated micromechanical parametric resonator. They experimentally obtained -4.9 dB of squeezing and theoretically predicted a lower bound of -6 dB noise squeezing at the parametric instability threshold with the parametric pump frequency set at twice the fundamental mode of the resonator. Only in 2013 this lower bound was surpassed by a lock-in feedback scheme developed by Vinante and Falferi in Ref. [8]. In this scheme, a -11.3 dB in squeezing of thermal fluctuations of a microscopic silicon beam cantilever was reached experimentally. Poot *et al.* [9] used the same squeezing technique with parametric pump and feedback that achieved noise compression at -15.1 dB in noise power reduction in an electro-optomechanical system. The same type of feedback scheme was applied to obtain strong squeezing in an optomechanical membrane [10], no new theoretical analysis was developed. The same feedback scheme and a similar analysis of the data as in Vinante and Falferi paper seems to have been used in Ref. [11]. Each one of these papers [8–11] makes important experimental advancements in the implementation of squeezing enhanced by feedback, nevertheless, a consistent stochastic theory of fluctuations squeezing with feedback is still missing.

Here we extend our previous work on squeezing of fluctuations in parametrically-modulated resonators with added noise [12] by including feedback. Specifically, we analyse and generalize the linear feedback scheme proposed by Vinante and Falferi to enhance squeezing of fluctuations. We believe our approach is more rigorous and more complete since we take into account detuning, we avoid using the averaging method to analyse the fluctuations in the frequency domain, but instead we Fourier transform the stochastic integro-differential equations of our model into an algebraic stochastic system in the frequency domain. We were able to obtain the dispersions in the sine and cosine quadratures at half the pump frequency. We also find that correlation arises

between these quadratures when there is detuning between half the pump frequency and the natural frequency of the resonator. Additionally, we also calculate the noise spectral density (NSD) of the resonators fluctuations. When the parametric resonator with feedback is excited by an added ac signal, without noise, we obtain the gain curve as a function of phase using the harmonic balance method. This analysis of a deterministic stationary response complements our stochastic analysis of squeezing. It is a simple way to check our results on squeezing.

The remainder of this paper is organized as follows. In Sec. II we initially analyse parametric amplification with two feedback schemes, and later, we propose and analyse an stochastic integro-differential model of enhanced fluctuations squeezing, cooling, and calculate the noise spectral density (NSD). In Sec. III we analyse and discuss our numerical results, and in Sec. IV we draw our conclusions.

II. THEORY

We will initially investigate the equation of motion of a parametrically-modulated resonator with lock-in feedback as proposed in Ref. [8], but driven by an external ac drive instead of white noise. This equation is given by

$$\ddot{x} + \gamma\dot{x} + \omega_0^2 x - F_p \sin(2\omega t)x = \eta u \sin \omega t + F_s \sin(\omega t + \phi), \quad (1)$$

where γ is the dissipation rate, ω_0 is the angular natural frequency of the resonator, F_p is the pump amplitude, 2ω is the pump frequency, η is the feedback constant, and u is the cosine quadrature of $x(t)$.

The alternative model of feedback that we propose is given by the following integro-differential equation

$$\ddot{x} + \gamma\dot{x} + \omega_0^2 x - F_p \sin(2\omega t)x = \frac{2\eta}{\tau} \int_{t-\tau}^t x(t') \cos(\omega t') dt' \sin \omega t + F_s \sin(\omega t + \phi), \quad (2)$$

where τ is the integration time span of a lock-in amplifier (it is also known as the time constant of the lock-in). We will see below that when τ is an integer multiple of $2\pi/\omega$ we recover the same gain obtained in the amplifier described by Eq. (1).

A. Phase-dependent amplification in the parametrically-driven resonator with lock-in feedback: averaging approach

Let us analyse the gain dependence on phase obtained from Eq. (1) in a similar way to what was performed by Rugar and Grütter in Ref. [7]. This analysis gives us insight on the response of this system to added noise. We now transform the fast variables $(x(t), \dot{x}(t))$ from Eq. (1) to the slow variables $(\mathcal{U}(t), \mathcal{V}(t))$ via $x(t) = \mathcal{U}(t) \cos \omega t - \mathcal{V}(t) \sin \omega t$ and $\dot{x}(t) = -\omega [\mathcal{U}(t) \sin \omega t + \mathcal{V}(t) \cos \omega t]$. Subsequently, we apply the averaging method to the equations of motion for $\mathcal{U}(t)$ and $\mathcal{V}(t)$ and obtain the following autonomous dynamical system

$$\begin{aligned} \dot{u} &= -\frac{\gamma}{2}u - \frac{1}{2\omega} \left[\left(\frac{F_p}{2} + \eta \right) u + \Omega v + F_s \cos \phi \right], \\ \dot{v} &= -\frac{\gamma}{2}v + \frac{1}{2\omega} \left(\Omega u + \frac{F_p}{2}v - F_s \sin \phi \right), \end{aligned} \quad (3)$$

where $\mathcal{U}(t) \approx u(t)$ and $\mathcal{V}(t) \approx v(t)$. For more details on the application of the averaging method see Ref. [13]. We can write the fixed-point solution of Eq. (3) as

$$\begin{pmatrix} u \\ v \end{pmatrix} = \frac{F_s}{\left(\frac{F_p}{2} + \gamma\omega + \eta \right) \left(\frac{F_p}{2} - \gamma\omega \right) - \Omega^2} \begin{pmatrix} \frac{F_p}{2} - \gamma\omega & -\Omega \\ -\Omega & \frac{F_p}{2} + \gamma\omega + \eta \end{pmatrix} \begin{pmatrix} -\cos \phi \\ \sin \phi \end{pmatrix} \quad (4)$$

Consequently, we can write the stationary squared amplitude $r^2 = u^2 + v^2$ as

$$\frac{r^2}{F_s^2} = \frac{\Omega^2 + \frac{F_p^2}{4} + \gamma^2\omega^2 + \frac{\eta^2}{2} + \eta \left(\frac{F_p}{2} + \gamma\omega \right) - [F_p\gamma\omega + \frac{\beta}{2}(\eta + F_p + 2\gamma\omega)] \cos 2\phi + \Omega(F_p + \eta) \sin 2\phi}{\left[\left(\frac{F_p}{2} + \gamma\omega + \eta \right) \left(\frac{F_p}{2} - \gamma\omega \right) - \Omega^2 \right]^2}. \quad (5)$$

Based on Eq. (5), we obtain that the instability threshold of parametric oscillator with lock-in feedback is given by

$$\frac{F_p^2}{4} - \gamma^2\omega^2 - \Omega^2 = -\eta \left(\frac{F_p}{2} - \gamma\omega \right). \quad (6)$$

From Eq. (5), we find the minimum and maximum amplitude of the response of the parametric amplifier at zero detuning ($\Omega = 0$) to be

$$\begin{aligned} r_{min}^2 &= \frac{F_s^2}{(F_p/2 + \gamma\omega + \eta)^2}, \\ r_{max}^2 &= \frac{F_s^2}{(F_p/2 - \gamma\omega)^2}. \end{aligned} \quad (7)$$

B. Phase-dependent amplification in the parametrically-driven resonator with lock-in feedback: harmonic balance approach

We now perform an analysis similar to the one developed in the previous subsection to obtain the phase-dependent gain of the driven parametric resonator with feedback whose dynamics is described by Eq. (2). We seek a stationary solution to this integro-differential equation in the form

$$x(t) = \frac{1}{2} [A(\omega)e^{-i\omega t} + A^*(\omega)e^{i\omega t}]. \quad (8)$$

Using the fact that the functions $e^{\pm i\omega t}$ are linearly independent, we find

$$\begin{aligned} (\omega^2 - \omega_0^2 - i\gamma\omega)A(\omega) - \frac{iF_p}{2}A^*(\omega) - \frac{i\eta}{2}(A + A^*) - \frac{\eta A}{8\tau\omega}(1 - e^{2i\omega\tau}) &= iF_s e^{-i\phi}, \\ \left[1 - \frac{i\eta\chi(\omega)}{2} - \frac{\eta\chi(\omega)}{4\tau\omega}(1 - e^{2i\omega\tau})\right]A(\omega) - \frac{i(F_p + \eta)\chi(\omega)}{2}A^*(\omega) &= i\chi(\omega)F_s e^{-i\phi}, \end{aligned} \quad (9)$$

which can be rewritten in the more compact form

$$\begin{aligned} a(\omega)A(\omega) - ib(\omega)A^*(\omega) &= i\chi(\omega)F_s e^{-i\phi}, \\ ib^*(\omega)A(\omega) + a^*(\omega)A^*(\omega) &= -i\chi^*(\omega)F_s e^{i\phi}, \end{aligned} \quad (10)$$

where

$$\begin{aligned} a(\omega) &= 1 - \frac{\eta\chi(\omega)}{2\tau} \left[\frac{(1 - e^{2i\omega\tau})}{2\omega} + i\tau \right], \\ b(\omega) &= \chi(\omega) \frac{F_p + \eta}{2}. \end{aligned}$$

Solving the algebraic system (10), we find

$$A(\omega) = \frac{ia^*(\omega)\chi(\omega)e^{-i\phi} + b\chi^*(\omega)e^{i\phi}}{|a(\omega)|^2 - |b(\omega)|^2} F_s. \quad (11)$$

If τ is a multiple of $2\pi/\omega$ we recover the amplification gain obtained with the averaging method in Eq. (5).

C. Parametrically-driven resonator with lock-in feedback and added noise

The Langevin equation of a damped parametrically driven oscillator with added noise and with feedback from the cosine quadrature output of a lock-in is given by

$$\ddot{x} + \gamma\dot{x} + \omega_0^2 x - F_p \sin(2\omega t)x = \frac{2\eta}{\tau} \int_{t-\tau}^t x(t') \cos(\omega t') dt' \sin \omega t + r(t). \quad (12)$$

By Fourier transforming Eq. (12), we obtain

$$\begin{aligned}
\tilde{x}(\nu) &= \chi(\nu)\tilde{r}(\nu) + \frac{F_p\chi(\nu)}{2i}[\tilde{x}(\nu+2\omega) - \tilde{x}(\nu-2\omega)] \\
&+ \frac{\eta\chi(\nu)}{\tau} \int_{-\infty}^{\infty} \left[\frac{e^{i(\nu+\omega)t}}{\nu+\omega} - \frac{e^{i(\nu-\omega)t}}{\nu-\omega} \right] \{x(t)\cos(\omega t) - x(t-\tau)\cos[\omega(t-\tau)]\} dt \\
&= \chi(\nu)\tilde{r}(\nu) + \frac{F_p\chi(\nu)}{2i}[\tilde{x}(\nu+2\omega) - \tilde{x}(\nu-2\omega)] \\
&+ \frac{\eta\chi(\nu)}{2\tau} \left[\frac{\tilde{x}(\nu+2\omega) + \tilde{x}(\nu)}{\nu+\omega} - \frac{\tilde{x}(\nu) + \tilde{x}(\nu-2\omega)}{\nu-\omega} \right] \\
&- \frac{\eta\chi(\nu)}{2\tau} \left\{ \frac{e^{i(\nu+\omega)\tau} [\tilde{x}(\nu+2\omega) + \tilde{x}(\nu)]}{\nu+\omega} - \frac{e^{i(\nu-\omega)\tau} [\tilde{x}(\nu) + \tilde{x}(\nu-2\omega)]}{\nu-\omega} \right\} \\
&= \chi(\nu)\tilde{r}(\nu) + \frac{F_p\chi(\nu)}{2i}[\tilde{x}(\nu+2\omega) - \tilde{x}(\nu-2\omega)] \\
&+ \frac{\eta\chi(\nu)}{2\tau} \left\{ \frac{[1 - e^{i(\nu+\omega)\tau}] [\tilde{x}(\nu+2\omega) + \tilde{x}(\nu)]}{\nu+\omega} - \frac{[1 - e^{i(\nu-\omega)\tau}] [\tilde{x}(\nu) + \tilde{x}(\nu-2\omega)]}{\nu-\omega} \right\}, \tag{13}
\end{aligned}$$

where we use the shorthand notation

$$\chi(\omega) = \frac{1}{\omega_0^2 - \omega^2 - i\gamma\omega}.$$

Here, we use the following notation for the Fourier transform

$$\tilde{f}(\nu) = \int_{-\infty}^{\infty} e^{i\nu t} f(t) dt.$$

1. Squeezing with feedback

At $\nu = \omega$, by neglecting off-resonance terms with $\tilde{x}(\pm 3\omega)$ in Eq. (13), we obtain

$$\begin{aligned}
&\left\{ 1 - \frac{\eta\chi(\omega)}{2\tau} \left[\frac{(1 - e^{2i\omega\tau})}{2\omega} + i\tau \right] \right\} \tilde{x}(\omega) - i\chi(\omega) \frac{\eta + F_p}{2} \tilde{x}^*(\omega) = \chi(\omega)\tilde{r}(\omega), \\
&i\chi^*(\omega) \frac{\eta + F_p}{2} \tilde{x}(\omega) + \left\{ 1 - \frac{\eta\chi^*(\omega)}{2\tau} \left[\frac{(1 - e^{-2i\omega\tau})}{2\omega} - i\tau \right] \right\} \tilde{x}^*(\omega) = \chi^*(\omega)\tilde{r}^*(\omega), \tag{14}
\end{aligned}$$

where we neglected the off-resonance terms with $\tilde{x}(3\omega)$. Solving this, we find

$$\tilde{x}(\omega) = \frac{a^*(\omega)\chi(\omega)\tilde{r}(\omega) + ib\chi^*(\omega)\tilde{r}^*(\omega)}{|a(\omega)|^2 - |b(\omega)|^2}, \tag{15}$$

where

$$\begin{aligned}
a(\omega) &= 1 - \frac{\eta\chi(\omega)}{2\tau} \left[\frac{(1 - e^{2i\omega\tau})}{2\omega} + i\tau \right], \\
b(\omega) &= \chi(\omega) \frac{F_p + \eta}{2}.
\end{aligned}$$

For the special case in which τ is an integer multiple of $2\pi/\omega$, this can be simplified to

$$\begin{aligned} a(\omega) &= 1 - \frac{i\eta\chi(\omega)}{2}, \\ b(\omega) &= \frac{F_p + \eta}{2}\chi(\omega). \end{aligned} \quad (16)$$

In this feedback scheme, we find that the instability threshold ($|a(\omega)| = |b(\omega)|$) is the same as the one obtained by the averaging method in Eq. (6).

The resonator response $\tilde{x}(\omega)$ given in Eq. (15) can be rewritten as

$$\tilde{x}(\omega) = \tilde{G}_0(\omega)\tilde{r}(\omega) + \Gamma(\omega)\tilde{r}^*(\omega), \quad (17)$$

where

$$\begin{aligned} \tilde{G}_0(\omega) &= \frac{a^*(\omega)\chi(\omega)}{|a(\omega)|^2 - |b(\omega)|^2} = \frac{\Omega + i(\gamma\omega + \eta/2)}{\Omega^2 + \gamma^2\omega^2 - F_p^2/4 + \eta(\gamma\omega - F_p/2)} \\ \Gamma(\omega) &= \frac{ib(\omega)\chi^*(\omega)}{|a(\omega)|^2 - |b(\omega)|^2} = \frac{i(F_p + \eta)/2}{\Omega^2 + \gamma^2\omega^2 - F_p^2/4 + \eta(\gamma\omega - F_p/2)}. \end{aligned} \quad (18)$$

In the following, we use the approach developed in Ref. [12] to analyse squeezing of fluctuations.

From Eq. (17), we find

$$\begin{aligned} \tilde{x}'(\omega) &= \tilde{G}'_0(\omega)\tilde{r}'(\omega) - \tilde{G}''_0(\omega)\tilde{r}''(\omega) + \Gamma'(\omega)\tilde{r}'(\omega) + \Gamma''(\omega)\tilde{r}''(\omega), \\ \tilde{x}''(\omega) &= \tilde{G}'_0(\omega)\tilde{r}''(\omega) + \tilde{G}''_0(\omega)\tilde{r}'(\omega) - \Gamma'(\omega)\tilde{r}''(\omega) + \Gamma''(\omega)\tilde{r}'(\omega), \end{aligned} \quad (19)$$

where the real and imaginary parts of \tilde{r} are \tilde{r}' and \tilde{r}'' , respectively. Using the parity properties of the Fourier transform of a real function

$$\begin{aligned} \tilde{r}'(\nu) &= \tilde{r}'(-\nu), \\ \tilde{r}''(\nu) &= -\tilde{r}''(-\nu), \end{aligned} \quad (20)$$

and the following statistical averages of white noise in the frequency domain:

$$\begin{aligned} \langle \tilde{r}'(\nu)\tilde{r}'(\nu') \rangle &= 2\pi D [\delta(\nu - \nu') + \delta(\nu + \nu')], \\ \langle \tilde{r}'(\nu)\tilde{r}''(\nu') \rangle &= 0, \\ \langle \tilde{r}''(\nu)\tilde{r}''(\nu') \rangle &= 2\pi D [\delta(\nu - \nu') - \delta(\nu + \nu')], \end{aligned} \quad (21)$$

At $\nu = \omega$, we obtain the two dispersions in quadrature and the correlation to be given by

$$\begin{aligned} \sigma_c^2(\omega) &= \lim_{\Delta\nu \rightarrow 0^+} \int_{\omega - \Delta\nu}^{\omega + \Delta\nu} \langle \tilde{x}'(\omega)\tilde{x}'(\nu') \rangle d\nu' \\ &= 2\pi D \left\{ |\tilde{G}_0(\omega)|^2 + |\Gamma(\omega)|^2 + 2 \operatorname{Re}\{\tilde{G}_0(\omega)\Gamma(\omega)\} \right\} \\ &= \frac{2\pi D [\Omega^2 + \gamma^2\omega^2 + F_p^2/4 - \gamma\omega F_p]}{[\Omega^2 + \gamma^2\omega^2 - F_p^2/4 + \eta(\gamma\omega - F_p/2)]^2}, \end{aligned} \quad (22)$$

$$\begin{aligned}
\sigma_s^2(\omega) &= \lim_{\Delta\nu \rightarrow 0^+} \int_{\omega-\Delta\nu}^{\omega+\Delta\nu} \langle \tilde{x}''(\omega) \tilde{x}''(\nu') \rangle d\nu' \\
&= 2\pi D \left\{ |\tilde{G}_0(\omega)|^2 + |\Gamma(\omega)|^2 - 2 \operatorname{Re}\{\tilde{G}_0(\omega)\Gamma(\omega)\} \right\} \\
&= \frac{2\pi D [\Omega^2 + (\gamma\omega + \eta/2)^2 + (F_p + \eta)^2/4 + (\gamma\omega + \eta/2)(F_p + \eta)]}{[\Omega^2 + \gamma^2\omega^2 - F_p^2/4 + \eta(\gamma\omega - F_p/2)]^2},
\end{aligned} \tag{23}$$

and

$$\begin{aligned}
\sigma_{cs}(\omega) &= \lim_{\Delta\nu \rightarrow 0^+} \int_{\omega-\Delta\nu}^{\omega+\Delta\nu} \langle \tilde{x}'(\omega) \tilde{x}''(\nu') \rangle d\nu' = 4\pi D \operatorname{Im}\{\tilde{G}_0(\omega)\Gamma(\omega)\} \\
&= \frac{2\pi D \Omega (F_p + \eta)}{[\Omega^2 + \gamma^2\omega^2 - F_p^2/4 + \eta(\gamma\omega - F_p/2)]^2},
\end{aligned} \tag{24}$$

where we used the relations

$$\begin{aligned}
\operatorname{Re}\{\tilde{G}_0(\omega)\Gamma(\omega)\} &= -\frac{(\gamma\omega + \eta/2)(F_p + \eta)/2}{[\Omega^2 + \gamma^2\omega^2 - F_p^2/4 + \eta(\gamma\omega - F_p/2)]^2}, \\
\operatorname{Im}\{\tilde{G}_0(\omega)\Gamma(\omega)\} &= \frac{\Omega(F_p + \eta)/2}{[\Omega^2 + \gamma^2\omega^2 - F_p^2/4 + \eta(\gamma\omega - F_p/2)]^2}.
\end{aligned} \tag{25}$$

In the important case of no detuning ($\Omega = 0$), we have

$$\begin{aligned}
\sigma_c^2(\omega) &= \frac{2\pi D [\gamma^2\omega^2 + F_p^2/4 - \gamma\omega F_p]}{[\gamma^2\omega^2 - F_p^2/4 + \eta(\gamma\omega - F_p/2)]^2} = \frac{2\pi D}{[\gamma\omega + F_p/2 + \eta]^2}, \\
\sigma_s^2(\omega) &= \frac{2\pi D [(\gamma\omega + \eta/2)^2 + (F_p + \eta)^2/4 + (\gamma\omega + \eta/2)(F_p + \eta)]}{[\gamma\omega + F_p/2 + \eta]^2 (\gamma\omega - F_p/2)^2} = \frac{2\pi D}{(\gamma\omega - F_p/2)^2},
\end{aligned} \tag{26}$$

$$\sigma_{cs}(\omega) = 0.$$

We can normalize these fluctuations by dividing them by the value $\sigma_0^2 = 2\pi D/(\gamma\omega)^2$ when $F_p = \eta = 0$. We find

$$\begin{aligned}
\sigma_c^2(\omega) &= \frac{\sigma_0^2}{(1+r+g)^2}, \\
\sigma_s^2(\omega) &= \frac{\sigma_0^2}{(1-r)^2},
\end{aligned} \tag{27}$$

where $r = F_p/(2\gamma\omega)$ and $g = \eta/(\gamma\omega)$. This result is equivalent to the one obtained in Eqs. (7). From the equations (27), we conclude that one can reach squeezing of σ_c as strong as possible by increasing the value of η with $F_p = 0$ while σ_s remains fixed at σ_0 . One limitation of this method is due to the fact that when increasing η the averaging method eventually breaks down. Furthermore, the approximation that led to equation (14) also breaks down since one has to take into account the off-resonance terms with $\tilde{x}(\pm 3\omega)$ in Eq. (13). For very high Q resonators, the

breakdown of this approximation is a minor issue though. With $r = 0$, the maximum gain is 1 and the squeezing in the cosine quadrature has no limit what leads to an overall cooling of the resonator. When $g = 0$ instead, the strongest squeezing occurs at $r \rightarrow 1$ with the lower limit being -6dB , what is in agreement with results of Rugar and Grutter [7] and Cleland [14], but in disagreement with the -3dB from Vinante and Falferi [8] and Poot *et al.* [9].

2. Noise spectral density

We can write Eq. (13) as

$$\begin{aligned} & \left\{ 1 - \frac{\eta\chi(\nu)}{2\tau} \left[\frac{1 - e^{i(\nu+\omega)\tau}}{\nu + \omega} - \frac{1 - e^{i(\nu-\omega)\tau}}{\nu - \omega} \right] \right\} \tilde{x}(\nu) \\ & + \frac{\chi(\nu)}{2} \left\{ -iF_p + \frac{\eta}{\tau} \frac{[1 - e^{i(\nu-\omega)\tau}]}{\nu - \omega} \right\} \tilde{x}(\nu - 2\omega) \\ & + \frac{\chi(\nu)}{2} \left\{ iF_p - \frac{\eta}{\tau} \frac{1 - e^{i(\nu+\omega)\tau}}{\nu + \omega} \right\} \tilde{x}(\nu + 2\omega) = \chi(\nu)\tilde{r}(\nu). \end{aligned} \quad (28)$$

We can rewrite the above equation as

$$A(\nu)\tilde{x}(\nu) + B^*(-\nu)\tilde{x}(\nu - 2\omega) + B(\nu)\tilde{x}(\nu + 2\omega) = \chi(\nu)\tilde{r}(\nu), \quad (29)$$

where we used the following shorthand expressions

$$\begin{aligned} A(\nu) &= 1 - \frac{\eta\chi(\nu)}{2\tau} \left[\frac{1 - e^{i(\nu+\omega)\tau}}{\nu + \omega} - \frac{1 - e^{i(\nu-\omega)\tau}}{\nu - \omega} \right], \\ B(\nu) &= \frac{\chi(\nu)}{2} \left[iF_p - \frac{\eta}{\tau} \frac{1 - e^{i(\nu+\omega)\tau}}{\nu + \omega} \right]. \end{aligned} \quad (30)$$

Near resonance ($\nu \approx \omega \approx \omega_0$), we can find an approximate closed system of equations

$$\begin{aligned} A(\nu - 2\omega)\tilde{x}(\nu - 2\omega) + B(\nu - 2\omega)\tilde{x}(\nu) &= \chi(\nu - 2\omega)\tilde{r}(\nu - 2\omega), \\ A(\nu + 2\omega)\tilde{x}(\nu + 2\omega) + B^*(-\nu - 2\omega)\tilde{x}(\nu) &= \chi(\nu + 2\omega)\tilde{r}(\nu + 2\omega), \end{aligned} \quad (31)$$

where we neglected terms with $\tilde{x}(\nu \pm 4\omega)$. With the help of these equations, we can write $\tilde{x}(\nu - 2\omega)$ and $\tilde{x}(\nu + 2\omega)$ in terms of $\tilde{x}(\nu)$, $\tilde{r}(\nu - 2\omega)$, and $\tilde{r}(\nu + 2\omega)$ as

$$\begin{aligned} \tilde{x}(\nu - 2\omega) &= \frac{1}{A(\nu - 2\omega)} [-B(\nu - 2\omega)\tilde{x}(\nu) + \chi(\nu - 2\omega)\tilde{r}(\nu - 2\omega)], \\ \tilde{x}(\nu + 2\omega) &= \frac{1}{A(\nu + 2\omega)} [-B^*(-\nu - 2\omega)\tilde{x}(\nu) + \chi(\nu + 2\omega)\tilde{r}(\nu + 2\omega)]. \end{aligned} \quad (32)$$

We replace $\tilde{x}(\nu - 2\omega)$ and $\tilde{x}(\nu + 2\omega)$ in Eq. (29) to obtain

$$\left[A(\nu) - \frac{B^*(-\nu)B(\nu - 2\omega)}{A(\nu - 2\omega)} - \frac{B(\nu)B^*(-\nu - 2\omega)}{A(\nu + 2\omega)} \right] \tilde{x}(\nu) = \chi(\nu)\tilde{r}(\nu) - \frac{B^*(-\nu)\chi(\nu - 2\omega)}{A(\nu - 2\omega)}\tilde{r}(\nu - 2\omega) - \frac{B(\nu)\chi(\nu + 2\omega)}{A(\nu + 2\omega)}\tilde{r}(\nu + 2\omega). \quad (33)$$

We can recast the approximate solution above in terms of elastic scattering, down, and up-conversions of the input noise as

$$\tilde{x}(\nu) = \mathcal{G}_0(\nu)\tilde{r}(\nu) + \mathcal{G}_+(\nu)\tilde{r}(\nu - 2\omega) + \mathcal{G}_-(\nu)\tilde{r}(\nu + 2\omega), \quad (34)$$

where

$$\begin{aligned} \mathcal{G}_0(\nu) &= \frac{\chi(\nu)}{A(\nu) - \frac{B^*(-\nu)B(\nu-2\omega)}{A(\nu-2\omega)} - \frac{B(\nu)B^*(-\nu-2\omega)}{A(\nu+2\omega)}}, \\ \mathcal{G}_+(\nu) &= -\frac{B^*(-\nu)\chi(\nu - 2\omega)}{A(\nu - 2\omega) \left[A(\nu) - \frac{B^*(-\nu)B(\nu-2\omega)}{A(\nu-2\omega)} - \frac{B(\nu)B^*(-\nu-2\omega)}{A(\nu+2\omega)} \right]}, \\ \mathcal{G}_-(\nu) &= -\frac{B(\nu)\chi(\nu + 2\omega)}{A(\nu + 2\omega) \left[A(\nu) - \frac{B^*(-\nu)B(\nu-2\omega)}{A(\nu-2\omega)} - \frac{B(\nu)B^*(-\nu-2\omega)}{A(\nu+2\omega)} \right]}. \end{aligned} \quad (35)$$

The NSD $S_{\tilde{x}}$ as defined in Ref. [15] is given by

$$S_{\tilde{x}}(\nu) = \lim_{\Delta\nu \rightarrow 0^+} \int_{\nu-\Delta\nu}^{\nu+\Delta\nu} \frac{\langle \tilde{x}(-\nu)\tilde{x}(\nu') \rangle}{2\pi} d\nu'. \quad (36)$$

When $\nu \neq \omega$, we find

$$S_{\tilde{x}}(\nu) = 2D [|\mathcal{G}_0(\nu)|^2 + |\mathcal{G}_+(\nu)|^2 + |\mathcal{G}_-(\nu)|^2], \quad (37)$$

where we used the fact that $\tilde{r}(\nu)$ is a white noise with zero mean and the statistical average $\langle \tilde{r}(\nu)\tilde{r}(\nu') \rangle = 4\pi D\delta(\nu + \nu')$.

III. RESULTS AND DISCUSSION

In Fig. 1 we plot the threshold lines of instability for several values of η in the first-order averaging approximation, given by Eq. (6) (solid lines), and of the integro-differential model, (discontinuous lines) which correspond to the zero of the denominator of Eq. (11). The discrepancy between the two models are due to the fact that implicitly the lock-in time constant is varied in the averaging model so that τ is an integer multiple of $2\pi/\omega$, whereas in the integro-differential model we use a fixed value of $\tau = 2\pi/\omega_0$. The latter case is easier to perform experimentally and also more

meaningful, since otherwise one has to vary three parameters (ω , F_p , and τ), instead of only two (ω and F_p), to trace the threshold line. It is noteworthy to mention that once there is feedback, the inversion symmetry $F_p \rightarrow -F_p$ is broken for the threshold lines. Because of this, the threshold line with $\eta = 0.5$ crosses $F_p = 0$ just above $\omega = 1$.

In Fig. 2 we plot the degenerate parametric amplification gain in dB with respect to the simple forced harmonic resonator response as a function of ϕ . As expected, when the lock-in time-constant τ is a multiple of $2\pi/\omega$ both models predict the same gain. In Fig. 3 we likewise plot the degenerate parametric amplification gain in dB with respect to the simple forced harmonic resonator response but with $\omega\tau/2\pi = 1.37$. These results cannot be reproduced by the averaged feedback model of Eq. (6). For the same values of F_p and η we obtain considerably stronger cooling, especially for the $\eta = 0.2$ and $\eta = 0.5$ curves. All pump amplitudes in both these figures are set at 90% of the threshold value.

In Fig. 4 we plot the minimal and maximal degenerate parametric amplification gain obtained from Eq. (5) as a function of pump amplitude with (a) $\omega/\omega_0 = 0.998$, (b) $\omega/\omega_0 = 1$, (c) $\omega/\omega_0 = 1.002$. As a comparison we plot in Fig. 5 the dispersions σ_c^2 and σ_s^2 along with the diagonalized dispersions σ_-^2 and σ_+^2 as a function of F_p with $\omega\tau/2\pi = 1$. For details on obtaining σ_- and σ_+ see Ref. [12]. As expected, the diagonalized dispersions behave very closely with the results plotted in Fig. 4.

In Fig. 6 we plot a color map of the strongest squeezing after diagonalization of the two-variable Gaussian probability distribution that generates the dispersions and correlation given in Eqs. (22)-(24). The strongest squeezing occurs in a narrow band around $\omega = \omega_0$. The value of τ is held constant at $\omega_0\tau/2\pi = 1$. As expected, there is little dependence of the squeezing on F_p since $g = 500$ and $r = 1$ at threshold from Eq. (27).

In Fig. 7 we plot the noise spectral density given by Eq. (37) for the variate $\tilde{x}(\nu)$ obtained from the Fourier transform of the integro-differential equation (12) with $\tau = 2\pi/\omega$. These results are beyond the scope of the model developed by Vinante and Falferi. Indeed, to the author's knowledge, this result is new in the scientific literature. We believe this measurement of the NSD is an important test for the theory, even more so than the squeezing estimates, since with it one can estimate the amount of cooling. Also, the squeezing measurements are made only at $\nu = \omega$, whereas the NSD is obtained across the spectrum of the resonator's response. In Fig. 8 we find considerably stronger cooling for the same parameters F_p and η as in the previous figure. We chose the value $\omega\tau/2\pi = 1.37$ that resulted in the strongest cooling.

The model of Vinante and Falferi is based on the application of the averaging method to a single-degree-of-freedom degenerate parametric amplifier at resonance ($\omega = \omega_0$). In their analysis, the authors replaced the single tone external drive by white noise and, subsequently, Fourier transformed the averaged equations. To our knowledge, there are several mathematical problems with this approach. The averaging method is usually applied to transform non-autonomous dynamical systems into slowly varying autonomous dynamical systems. For instance, if there is a zero-mean time-periodic parametric pump with period π/ω with $\omega \approx \omega_0$ in the original driven resonator, then only the Fourier component of the parametric pump at 2ω remain in the first-order averaged dynamical system, all higher harmonics are eliminated. If the resonator is also additively driven by a time periodic signal with period $2\pi/\omega$, then after averaging only the first Fourier component at ω will play a role, with all higher harmonics filtered out. Hence, the application of the averaging method works as a band-pass filter at $\omega \approx \omega_0$. So it seems there was an inconsistency in the analysis developed by Vinante and Falferi when applying the averaging method to a dynamical system driven by white noise. In their model, the averaged noise is still a white noise, with Fourier components with the same amplitude across the spectrum. In reality, the averaged noise should be a correlated noise. The Fourier analysis of an averaged dynamical system also seems contradictory, since high Fourier components will correspond to terms varying exceedingly fast in time. Finally, the averaged slow quadrature variables (X and Y in their notation) are related to the Fourier peak at ω_0 of \tilde{x} , that is $|\tilde{x}(\omega_0)| = \sqrt{X^2 + Y^2}$, hence the Fourier transform of $X(t)$ and $Y(t)$ does not seem mathematically meaningful. Here we avoided these issues by directly Fourier transforming Eq. (12) into the frequency domain, obtaining Eq. (13), which is exact. We proceeded by neglecting off-resonance terms such as $\tilde{x}(\pm 3\omega)$ in Eq. (15) to obtain squeezing or $\tilde{x}(\nu \pm 4\omega)$ in Eq. (34) in order to obtain an approximate expression for the NSD.

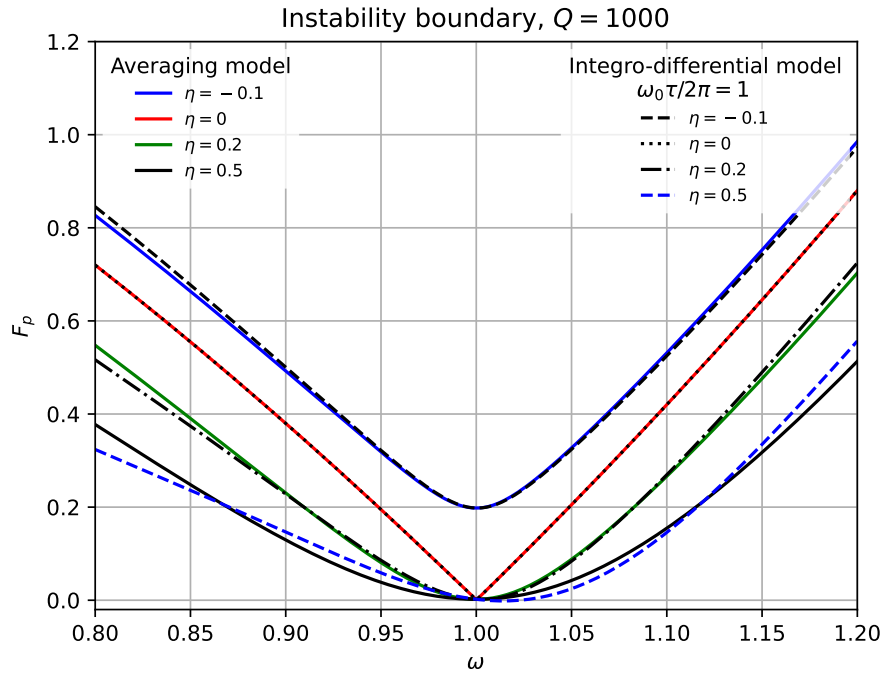


FIG. 1. Parametric instability thresholds for several values of the feedback constant η . The solid lines are obtained from Eq. (6), whereas the dashed or dotted lines are given by $|a(\omega)| = |b(\omega)|$ corresponding to the zero of the denominator of Eq. (11) for the fixed value of the lock-in time constant τ shown in the figure.

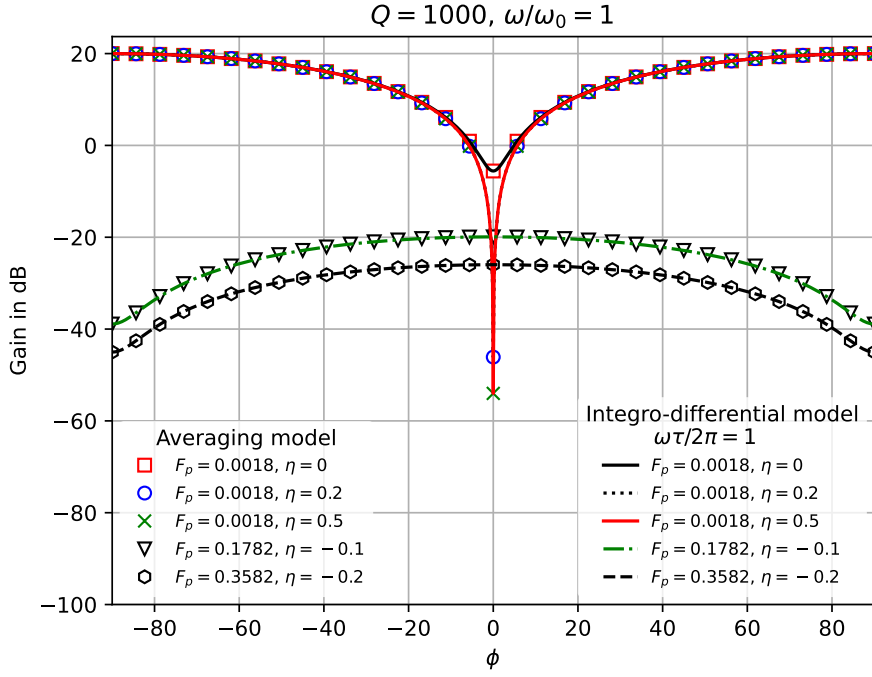


FIG. 2. Gain as a function of phase ϕ for a parametric amplifier with lock-in feedback. We plot the gain given by $20 \log_{10} \frac{r_{F_p, \eta}}{r_0}$, where the amplitude $r_{F_p, \eta}$ is the response of the parametric resonator with lock-in feedback and r_0 is the harmonic resonator response amplitude. The averaging model results are obtained from Eq. (5). The integro-differential model results are obtained from Eq. (11). All results with feedback yield deep deamplification (below -6 dB) at least in a narrow range around $\phi = 0$ for $\eta > 0$ and for all phases when $\eta < 0$.

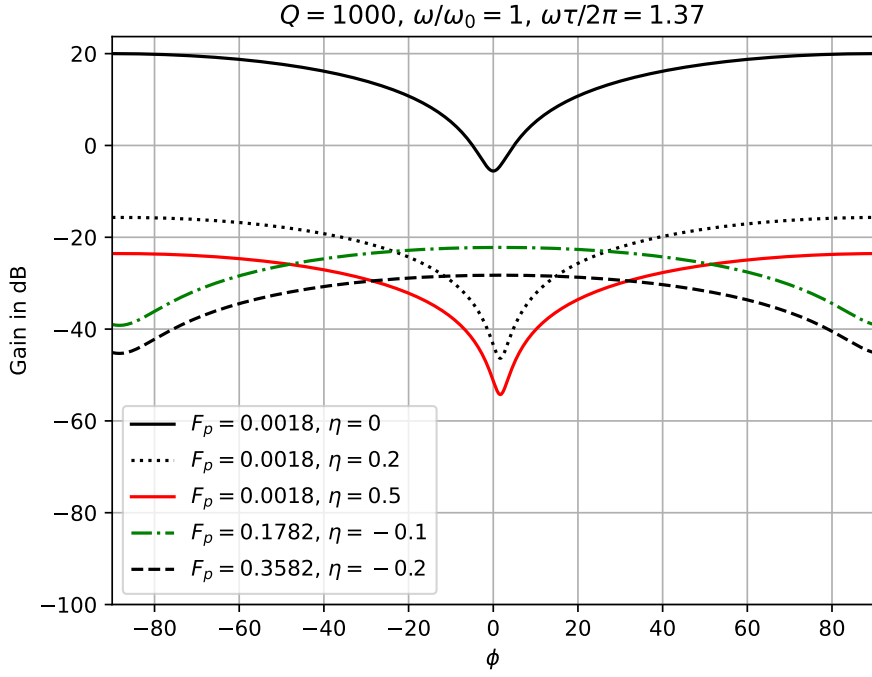


FIG. 3. Gain as a function of phase ϕ for a parametric amplifier with lock-in feedback. We plot the gain $20 \log_{10} \frac{r_{F_p, \eta}}{r_0}$ in decibels, where the amplitude $r_{F_p, \eta}$ is the response of the parametric resonator with lock-in feedback obtained from Eq. (11) with $\omega\tau/2\pi = 1.37$ and r_0 is the harmonic resonator response amplitude. We obtain considerably smaller gains than obtained in Fig. 2 with the same parameters except for the value of τ . For $\eta = 0.2$ and 0.5 , one obtains deamplification in all phases.

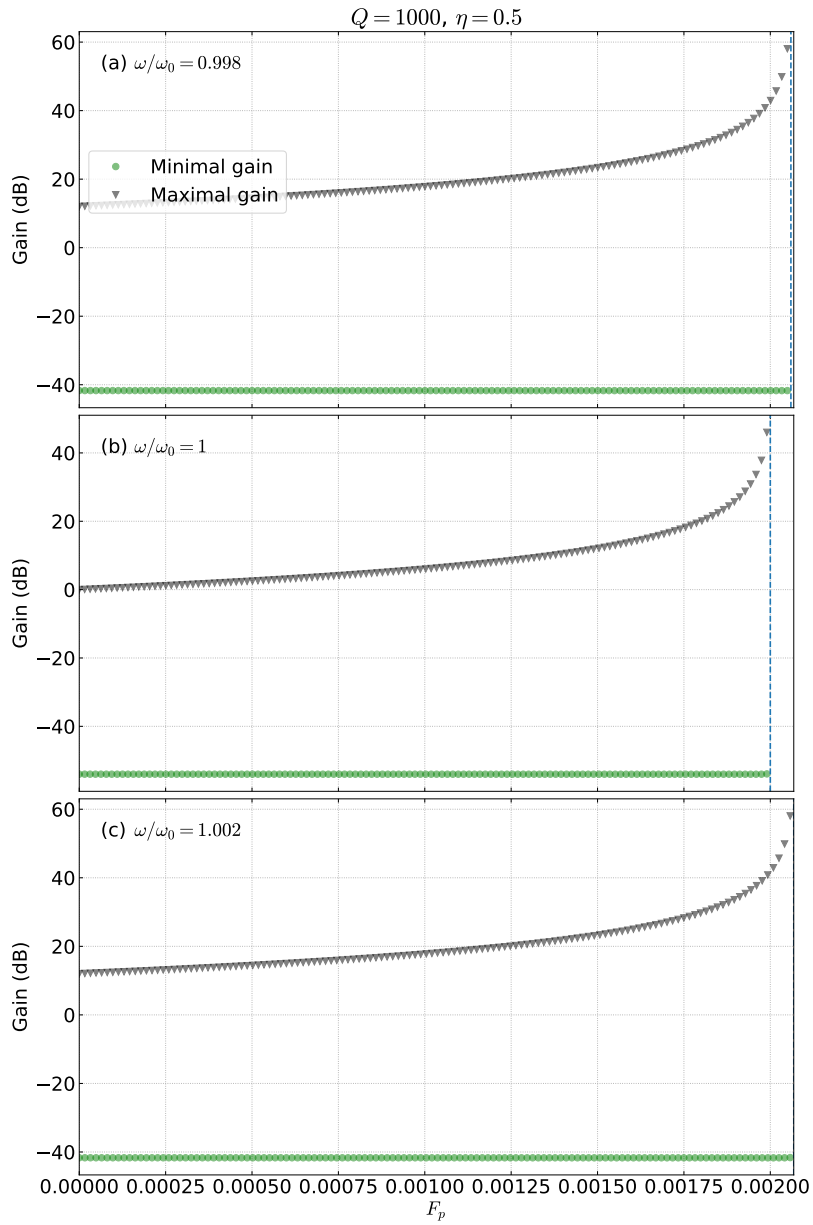


FIG. 4. Minimal and maximal gains as a function of pump amplitude. Here we use the same gain expression as in Fig. 2.

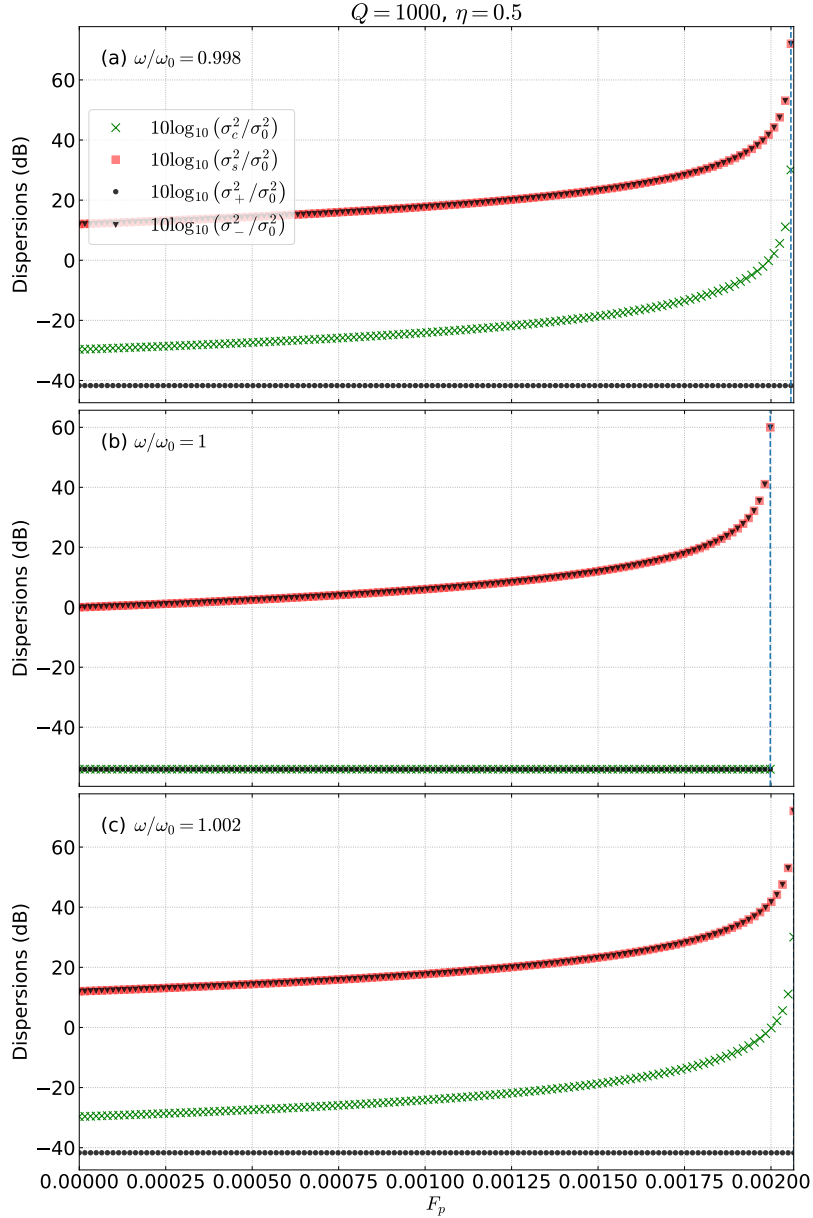


FIG. 5. Standard deviations: cosine quadrature (σ_c^2 from Eq. (22)), sine quadrature (σ_s^2 from Eq. (23)), and eigenvalues of the diagonalized covariance matrix (σ_-^2 and σ_+^2) in dB scale relative to the equilibrium values obtained at zero pump and zero feedback. Each plot ends very close to the instability threshold (vertical dashed lines). The common parameters used in all panels are given on top of the figure. In all panels we see that, unlike the single-degree-of-freedom parametric resonator without feedback, deep squeezing far below -6 dB can be achieved in the parametric resonator with feedback. The squeezing is practically independent of parametric modulation, but decreases with detuning. The diagonalized standard deviations are in agreement with the maximal and minimal gains depicted in Fig. 4. This indicates that our stochastic model is consistent with phase-dependent parametric amplification.

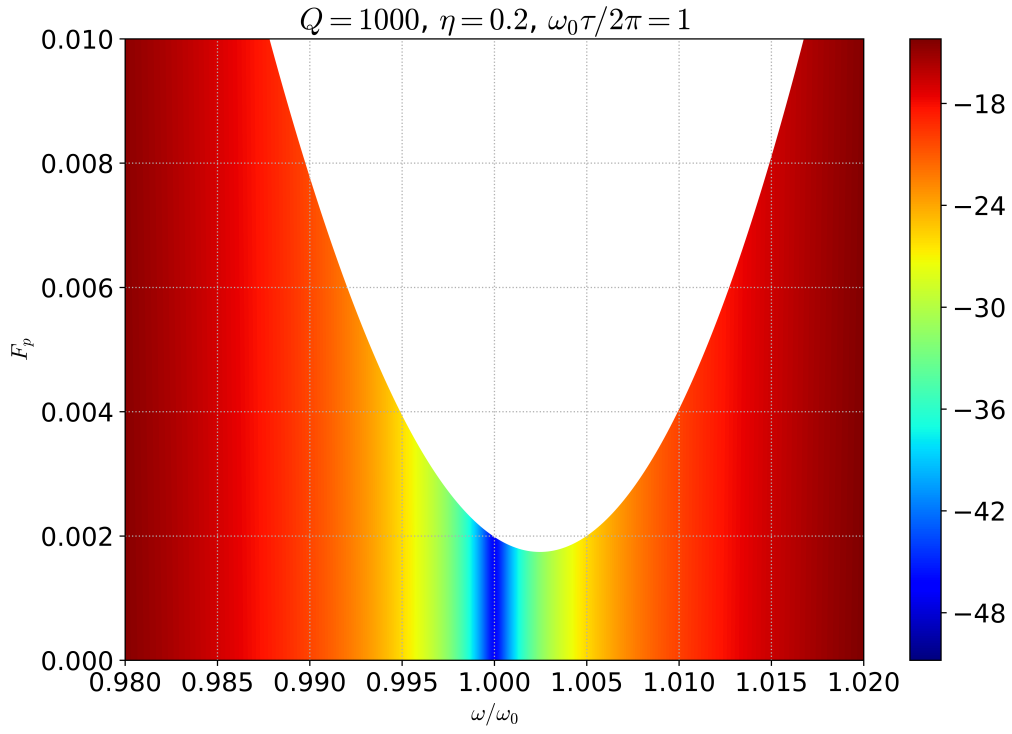


FIG. 6. Lock-in feedback minimum dispersion colormap in dB of the parametrically-driven amplifier. At each point in (ω, F_p) parameter space we plot the smallest dispersion obtained from the diagonalization of the covariance matrix with elements given in Eq. (22)-(24).

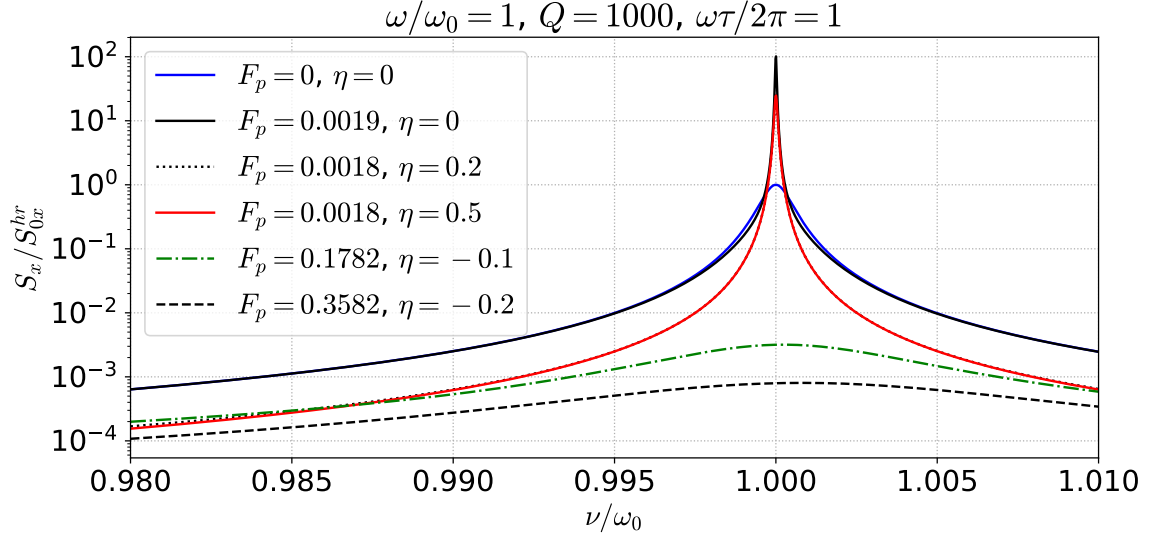


FIG. 7. Normalized noise spectral density lines obtained from Eq. (37) with $\tau = 2\pi/\omega$ for several values of F_p and η . All NSD's are divided by the peak value of the harmonic resonator NSD. The blue line is the NSD of the harmonic resonator, the solid black line corresponds to the NSD of the parametric resonator. The remaining lines correspond the parametric resonator with feedback. For $\eta > 0$, we see that the feedback does not alter the NSD of the parametric resonator near resonance in any significant way. On the other hand, far from resonance, the feedback response overrules the parametric response. As a comparison, the peak value of the curve with $F_p = 0$ and $\eta = 0.5$ is about $1/4$ of the peak value of the NSD of the harmonic resonator. There is substantial cooling only when $\eta < 0$.

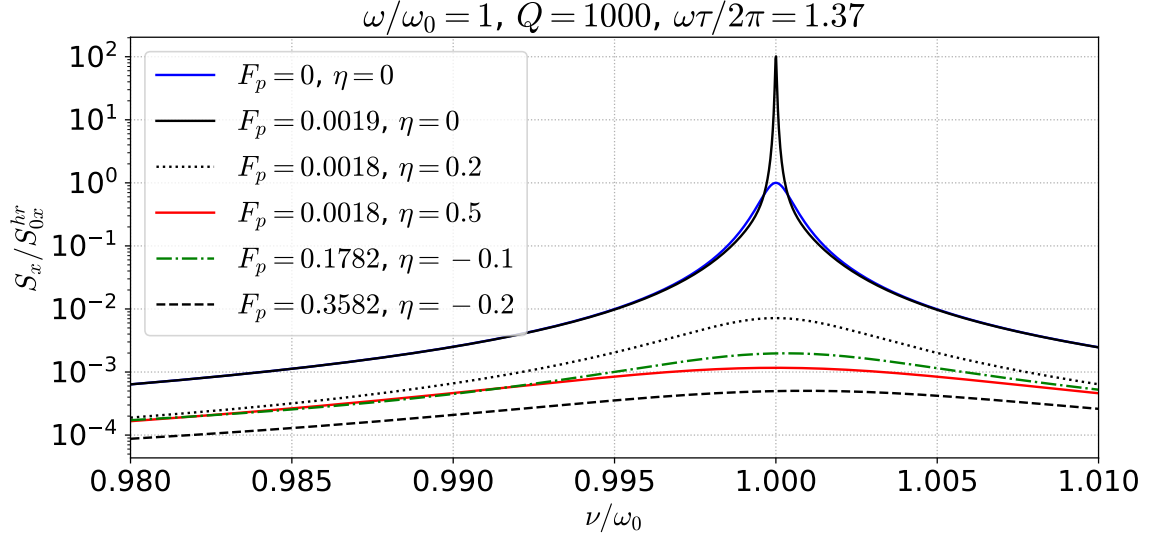


FIG. 8. Normalized noise spectral density curves with $\omega\tau/2\pi = 1.37$ for several values of F_p and η . The blue line is the NSD of the harmonic resonator, the solid black line corresponds to the NSD of the parametric resonator. We observe that there is cooling when there is feedback. When $\eta = 0.5$, the peak value of this curve is about 1.04×10^{-3} of the peak value of the NSD of the harmonic resonator. Even stronger cooling occurs when $\eta < 0$, but at the expense that F_p is set at a much higher value. These represent a far more substantial noise reduction than the ones achieved by the feedback scheme with $\tau = 2\pi/\omega$ plotted in Fig. 7.

IV. CONCLUSION

Here we developed a linear feedback scheme that is able to achieve squeezing and cooling of fluctuations in a resonator. The feedback scheme we proposed is described by an integro-differential equation, which in the most general form consists of an integral of the response of the resonator multiplied by a cosine and integrated over a given time interval. We believe our feedback scheme is more physical than the one proposed by Vinante and Falferi since it emulates the behavior of a lock-in amplifier. We can also easily account for a linear combination of u and v (the slowly varying averaged variables) in the feedback by changing the integration time τ of the lock-in amplifier. By doing so, we were able to achieve deeper squeezing and also stronger cooling for the same feedback constant than in Vinante and Falferi scheme.

Initially, we analysed the response of the resonator with feedback to an added ac signal without noise. When this feedback is applied to a harmonic resonator, it deamplifies its response with respect to the pure harmonic resonator response. When applied to a parametric resonator, one can obtain a strong dependence on phase, in some cases with amplification in one quadrature and deep deamplification in the other quadrature. Depending on the value of the feedback constant, one can also obtain deamplification in both quadratures, what leads to cooling. We verified that the phase-dependent gain obtained in Eq. (1) and Eq. (2) were the same when the lock-in time constant τ is a multiple of half the pump period.

We also investigated the response of the resonator (harmonic or parametric) with feedback to added white noise. Our model avoids the application of the averaging method in the presence of added noise. Instead, we analysed the stationary fluctuations of the resonator in the frequency domain. We observed that we can achieve deep squeezing far below the -6dB limit of pure parametric squeezing set by Rugar and Grutter's model. With our model, we were able to compute not only the squeezing at half the pump frequency, but also the NSD across a frequency band around resonance. We only added noise to the integro-differential model to avoid the issues of averaged dynamical systems with added noise. Instead of applying the averaging method, we Fourier analysed the original equations of motion (2).

In addition to squeezing, one can also obtain very strong cooling as evidenced by the reduction of the NSD by a factor of up to 10^4 . The calculation of the NSD allows for further experimental tests of our model. It would be very interesting to verify the amount of parameter space that is

available experimentally.

- [1] A. Bachtold, J. Moser, and M. Dykman, *Rev. of Mod. Phys.* **94**, 045005 (2022).
- [2] J. M. L. Miller, A. Ansari, D. B. Heinz, Y. Chen, I. B. Flader, D. D. Shin, L. G. Villanueva, and T. W. Kenny, *Applied Physics Reviews* **5** (2018).
- [3] C. Zhao, X. Zhou, M. Pandit, G. Sobreviela, S. Du, X. Zou, and A. Seshia, *Physical Review Applied* **12**, 044005 (2019).
- [4] J. Moser, J. Güttinger, A. Eichler, M. J. Esplandiu, D. Liu, M. Dykman, and A. Bachtold, *Nature nanotechnology* **8**, 493 (2013).
- [5] W. Zhang and K. L. Turner, *Sensors and Actuators A: Physical* **122**, 23 (2005).
- [6] L. Papariello, O. Zilberberg, A. Eichler, and R. Chitra, *Physical Review E* **94**, 022201 (2016).
- [7] D. Rugar and P. Grütter, *Phys. Rev. Lett.* **67**, 699 (1991).
- [8] A. Vinante and P. Falferi, *Phys. Rev. Lett.* **111**, 207203 (2013).
- [9] M. Poot, K. Y. Fong, and H. Tang, *New Journal of Physics* **17**, 043056 (2015).
- [10] S. Sonar, V. Fedoseev, M. J. Weaver, F. Luna, E. Vlieg, H. van der Meer, D. Bouwmeester, and W. Löffler, *Physical Review A* **98**, 013804 (2018).
- [11] A. Mashaal, L. Stefan, A. Ranfagni, L. Catalini, I. Chernobrovkin, T. Capelle, E. Langman, and A. Schliesser, [arXiv:2403.02328](https://arxiv.org/abs/2403.02328) (2024).
- [12] A. A. Batista, R. S. Moreira, and A. de Souza, [arXiv:2404.03758](https://arxiv.org/abs/2404.03758) (2024).
- [13] A. A. Batista, *Phys. Rev. E* **86**, 051107 (2012).
- [14] A. N. Cleland, *New Journal of Physics* **7**, 235 (2005).
- [15] A. A. Batista, A. A. L. de Souza, and R. S. N. Moreira, *Journal of Applied Physics* **132**, 174902 (2022).